Hindawi
Computational Intelligence and Neuroscience
Volume 2023, Article ID 4765891, 14 pages
https://doi.org/10.1155/2023/4765891

*Research Article*

# An Improved Adam Optimization Algorithm Combining Adaptive Coefficients and Composite Gradients Based on Randomized Block Coordinate Descent

**Miaomiao Liu,[1,2] Dan Yao,[1] Zhigang Liu,[1,2] Jingfeng Guo,[3] and Jing Chen[3]**

[1]*School of Computer and Information Technology, Northeast Petroleum University, Daqing 163318, China*
[2]*Heilongjiang Key Laboratory of Petroleum Big Data and Intelligent Analysis, Daqing 163318, China*
[3]*College of Information Science and Engineering, Yanshan University, Qinhuangdao 066004, China*

Correspondence should be addressed to Dan Yao; 15735104623@163.com

Received 22 September 2022; Revised 28 December 2022; Accepted 2 January 2023; Published 10 January 2023

Academic Editor: Upaka Rathnayake

An improved Adam optimization algorithm combining adaptive coefficients and composite gradients based on randomized block coordinate descent is proposed to address issues of the Adam algorithm such as slow convergence, the tendency to miss the global optimal solution, and the ineffectiveness of processing high-dimensional vectors. The adaptive coefficient is used to adjust the gradient deviation value and correct the search direction firstly. Then, the predicted gradient is introduced, and the current gradient and the first-order momentum are combined to form a composite gradient to improve the global optimization ability. Finally, the random block coordinate method is used to determine the gradient update mode, which reduces the computational overhead. Simulation experiments on two standard datasets for classification show that the convergence speed and accuracy of the proposed algorithm are higher than those of the six gradient descent methods, and the CPU and memory utilization are significantly reduced. In addition, based on logging data, the BP neural networks optimized by six algorithms, respectively, are used to predict reservoir porosity. Results show that the proposed method has lower system overhead, higher accuracy, and stronger stability, and the absolute error of more than 86% data is within 0.1%, which further verifies its effectiveness.

## 1. Introduction

The introduction of this study is described in the following sections.

*1.1. Background.* With the rapid development of artificial intelligence, population optimization algorithms [1], the memetic algorithm [2], and first-order optimization methods, such as random gradient descent [3] and gradient descent with momentum (SGDM) [4], have been widely used in the field of machine learning and play an important role in solving optimization problems of complex systems. As a first-order adaptive step stochastic gradient optimizer, the Adam algorithm has gained a lot of attention in the field of numerical optimization for its outstanding computational efficiency and has been widely used in deep learning with impressive results [5]. However, the first-order momentum of the Adam algorithm is an exponentially weighted average of the historical gradients, and the update of the search direction is influenced by the deviation value of the gradient, which leads to slow convergence of the model. While the second-order momentum is accumulated over a fixed time window, and the data do not vary monotonically with the time window. This generates oscillations in the learning rate in the later stages of training and leads to failure of the model convergence. Therefore, it has become a focus of researchers to seek methods to improve the defects of the Adam algorithm in convergence.

*1.2. Related Work.* The Adam algorithm mainly uses momentum and deviation correction methods to achieve stronger search ability. Hence, most of the relevant research studies focus on further improving the performance of the optimizer or combining it with other optimization methods [6]. By assigning a "long-term memory" to the historical gradients, the AMSGrad [7] algorithm is proposed, which solves the convergence problem theoretically. Based on the momentum-accelerated stochastic gradient descent, Ma and Yarats [8] proposed a quasi-hyperbolic weight decay acceleration algorithm and adjusted the hyperparameters. Luo et al. [9] compared the generalization and convergence capabilities of stochastic gradient descent (SGD) and adaptive methods and provided new variants of Adam and AMSGrad, identified as AdamBound and AMSBound, respectively, by using dynamic learning rate variation bounds to achieve an asymptotic and smooth transition from adaptive methods to SGD. Yin et al. [10] proposed a C-Adam algorithm based on the current gradient, predicted gradient, and historical momentum gradient to attain iteratively more accurate search directions by updating the true gradient. Subsequently, a hybrid Adam-based optimization method HyAdamC [11] is proposed, which carefully tunes the search intensity using three-speed control functions: initial, short term, and long term, thus, significantly enhancing the prediction accuracy. Later, some methods were proposed such as AdaGrad [12], Yogi [13], Fromage [14], diffGrad [15], RBC-Adam [16], and TAdam [17].

Although the above optimization algorithms can achieve competent results when used to train neural networks, they still pose the following three problems. First, the algorithms need to determine an optimal search speed at each training step, which may introduce overfitting or affect the training accuracy and testing accuracy [18]. Secondly, the current momentum used in the Adam is prone to inaccurate search directions because of gradient deviations caused by the outliers [17]. Thirdly, such algorithms have difficulty in identifying the current state of the optimized terrain in the solution space spanned by the weights, and therefore, they fail to find the approximate optimal weights.

*1.3. Contribution.* To deal with the above problems, an improved Adam optimization algorithm, combining adaptive coefficients and composite gradients based on randomized block coordinate descent, written ACGB-Adam, is proposed. The contributions and innovations of this article are summarized as follows. (1) To deal with the problem of slow convergence of the Adam algorithm, adaptive coefficients are used for computing the degree of difference between the first-order momentum and the current gradient. This helps to reduce the degree of influence of parameters on the deviated gradient caused by the outlier points, improve the proportion of influence of the parameters on the momentum at the previous moment, avoid the gradient deviation, and enhance the search speed and convergence accuracy. (2) Aiming at the shortcoming that the Adam algorithm tends to miss global optimal solution, the prediction gradient is introduced and combined with the current gradient and the first-order momentum to form a composite gradient, thus, providing a joint determination of the direction of the iterative optimization. This helps to get a more accurate search direction and improve the global search capability, thereby speeding up the search for the global optimal solution. (3) To address the issue of dealing with high-dimensional vectors and the high computational overhead of the Adam algorithm, the randomized block coordinate descent (RBC) is introduced to determine the gradient update mode according to the random variables of the diagonal matrix. This ensures that only one block of the gradient needs to be computed in each iteration instead of the entire gradient. Then, the dynamic balance between the convergence accuracy and the system overhead can be achieved. (4) Combining the above ideas, the ACGB-Adam optimization algorithm is proposed. The optimization performance of the proposed algorithm is verified by standard classification datasets Mnist and CIFAR-10, which is further applied to BP neural networks and compared with optimization methods based on SGD, AdaGrad, Adam, C-Adam, and RBC-Adam. From the experimental results, it can be concluded that the algorithm proposed in this article has better performance, and its convergence speed, stability, and prediction accuracy are higher than those of the other five methods.

## 2. Adam Algorithm

The Adam algorithm is explained in the following sections.

*2.1. Basic Principles.* The Adam algorithm [19] differs significantly from the traditional SGD algorithms. SGD algorithm maintains a single learning rate to update all the weights during training; the AdaGrad algorithm reserves a learning rate for each parameter to improve the performance on sparse gradients; the RMSProp algorithm adaptively reserves a learning rate for each parameter based on the mean of the nearest magnitude of the weight gradient, thereby improving the algorithm's performance on nonstationary problems. Adam algorithm sets independent adaptive learning rates for different parameters by computing the first-order and the second-order momentum estimates of the gradient and gains the advantages of both the AdaGrad and RMSProp algorithms.

Particularly, the Adam algorithm uses not only first-order momentum to maintain the direction of the historical gradient but also second-order momentum to maintain the adaptive state of the learning rate. Besides, it directly considers a sequential setting where samples are displayed sequentially rather than assuming that a large number of training samples are preavailable. Because of these reasons, the Adam algorithm performs well with high computational efficiency and low memory requirements [20]. In recent years, research on the Adam algorithm has flourished, and several variants such as NAdam [21], GAdam [22], AMSGrad [23], Adafactor [24], and Adadelta [25] have been proposed.

*2.2. Algorithm Flow.* In view of accurately describing the Adam algorithm and its improvement, the relevant parameters involved in this article are described in Table 1. The pseudocode of the Adam algorithm is shown in Algorithm 1.

*2.3. Existing Problems.* In deep learning, the Adam algorithm is widely used to solve parameter optimization problems because of its efficient calculation, smaller number of tuning parameters, and high compatibility. However, there are certain shortcomings of this algorithm. Firstly, the model convergence speed is very slow. The first-order momentum in the Adam algorithm is the exponentially weighted average of the historical gradient, which controls the update of the optimization direction. It gets easily affected by the gradient deviation value, leading to poor searchability and slow convergence speed of the model. Secondly, it is easy to miss the global optimal solution. The neural network model often contains a large number of parameters. In a space with extremely high dimensions, the nonconvex objective function often tends to rise and fall, and it is easy to produce the "plateau phenomenon" that causes the training to stop and then miss the global optimal solution.

## 3. ACGB-Adam Algorithm

To solve the problems of the Adam algorithm, the ACGB-Adam algorithm is proposed, which is primarily improved from the following three aspects. (1) To address the slow convergence speed of the Adam algorithm, an adaptive coefficient calculation method is adopted to improve the search direction and reduce the influence of gradient deviation caused by the outliers on the first-order momentum search direction. (2) In view of the issue that the Adam algorithm is easy to miss the global optimal solution, a composite gradient is formed out of the current gradient and the predicted gradient, which enhances the correctness of the search direction, improves the global optimization ability, and further boosts the search efficiency and optimization ability of the algorithm. (3) To reduce the computational cost of the algorithm, the randomized block coordinate descent method is introduced to select variables by modules to calculate the gradient update mode. This contributes to reducing the memory and CPU utilization as much as possible on the premise of ensuring the search performance.

*3.1. Adjust Gradient Deviation with Adaptive Coefficients.* In the Adam algorithm, the gradient deviation caused by outliers has a significant impact on the calculation of the first-order momentum. From the exponential weighted average (EWA), it can be noticed that the first-order momentum maintains the movement direction of its historical gradient, so the search direction of the next time is determined by the previous first-order momentum of the current gradient. Subsequently, if the current gradient is far from the global optimal direction, the direction of the first-order momentum will be further away from the approximate optimum, leading to a serious decline in the search ability. Figure 1 demonstrates the impact of the desired gradient on the first-order momentum. As highlighted in Figure 1(a), the first-order momentum at the current time $m_t$ is calculated by the EWA between the previous momentum $m_{t-1}$ and the current gradient $g_t$, and the two constant coefficients $\beta_1$ and $(1-\beta_1)$ are used to obtain the EWA. At this time, the direction of $m_t$ shifts to the direction of $g_t$ if $g_t$ deviates from the desired direction due to the influence of the outliers. Therefore, the search direction at the next time will also be further away from the approximate global optimum $P^*$, as demonstrated in Figure 1(b).

To improve the slow convergence speed caused by the deviation of the first-order momentum search direction, it is mandatory to confirm whether the current gradient is the deviation gradient caused by the outliers and reduce its impact as much as possible. So, the ACGB-Adam algorithm computes the difference between $m_{t-1}$ and $g_t$. If this difference is very large, $g_t$ is more likely to affect the search direction at the next moment than the first-order momentum. In this case, the influence of the momentum at the previous time $m_{t-1}$ will be increased according to their difference degree by an adaptive coefficient to reduce the influence of $g_t$ on $m_t$ as much as possible. The outlier gradient adjustment method based on the adaptive coefficient is expressed as

$$m_t = \beta_{1,t} m_{t-1} + \left(1-\beta_{1,t}\right) g_t, \tag{1}$$

where $\beta_{1,t}$ is the adaptive coefficient, which is proportional to the difference between $m_{t-1}$ and $g_t$, namely, $\beta_{1,t} \propto |m_{t-1} - g_t|$. In this article, the method in [17] is used to determine the difference ratio, as mentioned in equation (2). In equation (2), $q_t$ denotes the similarity between $g_t$ and $m_t$ as calculated by equation (3), and $d$ represents the vector dimension. $Q_{t-1}$ is a weighted cumulative sum of $q_1$, $q_2$ ,..., $q_{t-1}$, as calculated by equation (4):

$$\beta_{1,t} = \frac{Q_{t-1}}{Q_{t-1} + q_t}, \tag{2}$$

$$q_t = 2d\left(d + \sum_{j=1}^{d} \frac{\left(g_{t,j} - m_{t-1,j}\right)^2}{v_{t-1,j}}\right), \tag{3}$$

$$Q_{t-1} = \frac{2\beta_1 - 1}{\beta_1} Q_{t-2} + q_{t-1}. \tag{4}$$

*3.2. Combined Predicted Gradient to Form Composite Gradient.* In the Adam algorithm, the first-order momentum $m_t$ is determined by the current gradient $g_t$ and the historical first-order momentum $m_{t-1}$. This causes the search direction to be excessively dependent on the historical gradient, making it easy to miss the global optimum. The ACGB-Adam algorithm thus introduces the predicted gradient $u_t$, updates the parameter to be optimized at the next moment by the gradient descent method, and differs it from the historical momentum so that it uses a real gradient update and then merges with the current gradient and the historical first-order momentum to form a composite gradient. This makes it possible to get a more accurate search direction in the next iteration. Figure 2 illustrates the schematic diagram of the

TABLE 1: Description of parameters of Adam algorithm and its improvement.

| Parameters | Description |
|---|---|
| $\alpha$ | Learning rate |
| $\beta_1, \beta_2$ | Exponential decay rate of the first-order and second-order moment estimation, respectively |
| $T,\ t$ | The maximum iterations and the current $t$ time step, respectively |
| $\beta_1^t, \beta_2^t$ | Product of exponential decay rate of the first and second-order moment estimation at $t$ time step, respectively, $(1-\beta_1)\sum_{i=1}^t \beta_1^{t-i} = 1-\beta_1^t$ and $(1-\beta_2)\sum_{i=1}^t \beta_2^{t-i} = 1-\beta_2^t$ |
| $m_t$ | The first-order moment vector at $t$ time step |
| $v_t$ | The second-order moment vector at $t$ time step |
| $g_t$ | Current gradient at $t$ time step |
| $\beta_{1,t}$ | Adaptive coefficient |
| $u_t$ | Prediction gradient |
| $D_t$ | Random diagonal matrix at $t$ time step |
| $d_i^t$ | The $i$th diagonal element of $D_t$ with independent identical Bernoulli distribution |
| $\theta_t$ | The parameter that needs to be optimized |
| $f_t$ | The sequence of the smooth convex loss function |
| $P^*$ | Global optimal position |

```
Input: $\alpha, \beta_1, \beta_2, f_t$
Output: $\theta_t$
(1)  Initialize parameters ($\alpha = 0.001$, $\beta_1 = \beta_2 = 0.9$, $m_0 = 0$, $v_0 = 0$, $t = 0$)
(2)    For $t = 1$ to $T$ do
(3)      Get a stochastic gradient objective at time step $t$: $g_t = \nabla_\theta f_t(\theta_{t-1})$
(4)      Update biased first-order moment estimation: $m_t = \beta_1 m_{t-1} + (1-\beta_1) g_t$
(5)      Update biased second-order moment estimation: $v_t = \beta_2 v_{t-1} + (1-\beta_2) {g_t}^2$
(6)      Get bias-corrected first-order moment estimation: $\widehat{m_t} = m_t/(1-\beta_1^t)$
(7)      Get bias-corrected second-order moment estimation: $\widehat{v_t} = v_t/(1-\beta_2^t)$
(8)      Update the parameter: $\theta_t = \theta_{t-1} - \alpha\widehat{m_t}/\sqrt{\widehat{v_t}}$
(9)    End For
(10) Return $\theta_t$
```

ALGORITHM 1: Adam.

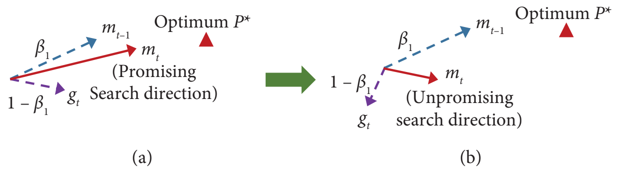

FIGURE 1: The effect of the desired gradient on the first-order momentum: (a) ordinary gradients and (b) outlier gradients.

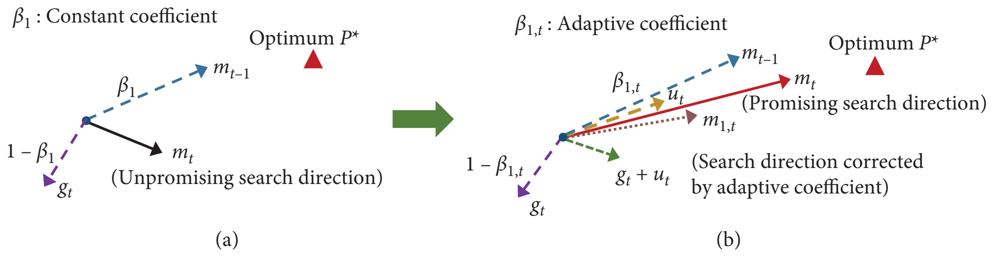
$\beta_1$ : Constant coefficient
Optimum $P^*$
$\beta_1$
$m_{t-1}$
$1-\beta_1$
$m_t$
$g_t$
(Unpromising search direction)
$\beta_{1,t}$ : Adaptive coefficient
$\beta_{1,t}$
$u_t$
$m_t$
(Promising search direction)
$m_{1,t}$
$1-\beta_{1,t}$
$g_t + u_t$
(Search direction corrected by adaptive coefficient)
(a)
(b)

FIGURE 2: Adjustment of the first-order momentum based on adaptive coefficient and composite gradient: (a) ordinary gradient optimization and (b) the improved gradient optimization.

first-order momentum search direction adjustment mechanism integrating adaptive coefficients and composite gradient.

For the first-order momentum before improvement in Figure 2(a), a constant coefficient $\beta_1$ is used. Therefore, if $g_t$ moves away from the optimal position $P^*$ in a direction

```
Input: $\theta_0 \epsilon R^N$ ($R^N$ is a $N$-dimensional set of real numbers)
Output: $\theta_t$
(1)    Initialize parameters $\theta = \theta_0$
(2)    For $t = 1$ to $T$ do
(3)        $t = t + 1$
(4)        Select coordinates $i \epsilon \{1, 2, ..., N\}$ evenly and randomly
(5)        Update $\theta_t^{(i)} = \theta_{t-1}^{(i)} - 1/L_i \nabla_\theta f_i(\theta_{t-1})$ where $L_1, L_2, ..., L_N$ are Lipschitz constants
(6) End For
```

Algorithm 2: Randomized block coordinate descent (RBC).

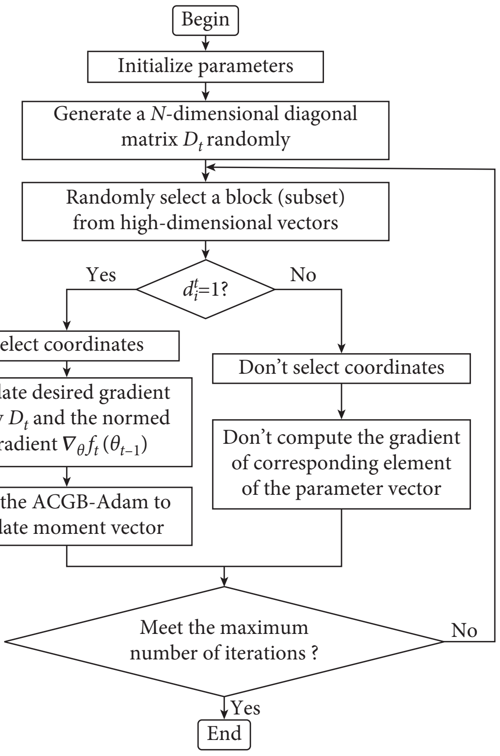
Begin
Initialize parameters
Generate a $N$-dimensional diagonal matrix $D_t$ randomly
Randomly select a block (subset) from high-dimensional vectors
$d_i^t$=1?
Yes
No
Select coordinates
Update desired gradient $g_t$ by $D_t$ and the normed gradient $\nabla_\theta f_t(\theta_{t-1})$
Use the ACGB-Adam to update moment vector
Don't select coordinates
Don't compute the gradient of corresponding element of the parameter vector
Meet the maximum number of iterations ?
No
Yes
End

Figure 3: Flowchart of the gradient calculation based on RBC.

deviated from the desired direction, $m_t$ will continue its movement in the direction of $g_t$. In Figure 2(b), $m_{1,t}$ is the search direction corrected by the adaptive coefficient $\beta_{1,t}$. As compared to the direction of $m_t$ in Figure 2(a), $m_{1,t}$ will approach the global optimal position in a more accurate direction. Therefore, to adjust the gradient effect of outliers, an adaptive coefficient is introduced. Because of this, the influence of the outliers of the first-order momentum at the previous moment is as small as possible while calculating the current first-order momentum. Thus, a more potential search direction can be effectively determined, and the search for the global optimal solution can be accelerated. Secondly, based on the use of an adaptive coefficient to correct the search direction, the predicted gradient $u_t$ is introduced, and the search direction $m_t$ is formed together with the current gradient $g_t$ and the historical first-order momentum $m_{t-1}$. It can be observed that, by introducing the predicted gradient, on the basis of the adjustment of $m_{1,t}$, the search direction formed can be further closer to $P^*$ to avoid missing the global optimal solution. Therefore, the convergence accuracy of the algorithm is improved.

### 3.3. Gradient Update Mode Based on Randomized Block Coordinate Descent.

*3.3. Gradient Update Mode Based on Randomized Block Coordinate Descent.* As a simple and effective method, SGD is often used to learn linear classifiers. However, when dealing with high-dimensional vector data, the full gradient descent mode in SGD is not easy to be implemented in parallel. Therefore, this article introduces the random block coordinate method to optimize the Adam algorithm, which can not only handle high-dimensional vectors but also can avoid calculating the complete gradient of all dimensional data in each iteration, thus saving the computing cost and reducing the system overhead on the premise of ensuring the convergence speed and optimization accuracy.

*3.3.1. RBC Algorithm.* RBC is a random optimization algorithm [26]. In each iteration, a coordinate (block) is randomly selected, and its variables are updated in the coordinate gradient direction. If $f$ is a convex smooth function and its gradient $L_i$ ($i \epsilon \{1, 2, ..., N\}$) is a Lipschitz continuous number, the flow of the RBC algorithm is as follows: wherein, $x_t$ denotes the parameter vector to be updated. The RBC algorithm is as shown in Algorithm 2.

RBC algorithm has been widely used to address large-scale optimization problems because of its low computation and update cost [16] and its good optimization effect. For instance, Hu and Kwok [27] studied the learning of scalable nonparametric low-rank kernels, and Zhao et al. [28] proposed an accelerated small-batch random block optimization algorithm. Moreover, several machine learning algorithms can be optimized with the help of RBC. For instance, Singh et al. [29] improved the gradient projection algorithm by using RBC, and Xie et al. [30] combined the RBC algorithm with mean-variance optimization.

*3.3.2. Gradient Calculation Based on RBC.* In this article, a new gradient calculation method is proposed based on the RBC method. Let $D_t$ ($t = 0, 1, 2, ..., N$) be a $n$-dimensional diagonal matrix in the $t$th iteration, and the $i$th element on the diagonal is denoted as $d_i^t$. Here, $d_i^t$ is a Bernoulli random variable that satisfies the independent identically distributed, i.e., $d_i^t \in \{0, 1\}, 1 \le i \le N$:

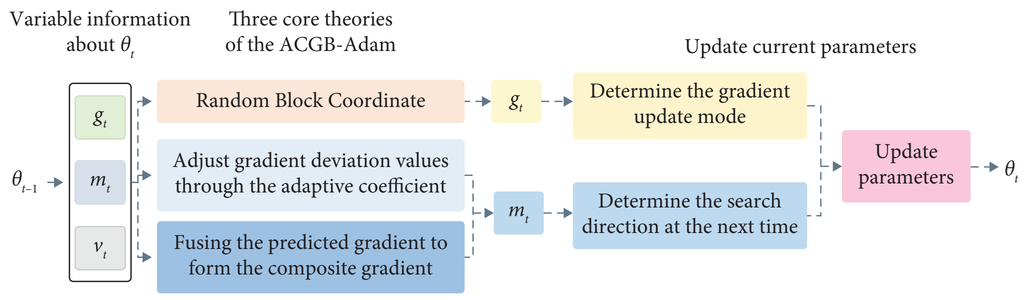
Variable information about $\theta_t$
Three core theories of the ACGB-Adam
Update current parameters
$\theta_{t-1}$
$g_t$
$m_t$
$v_t$
Random Block Coordinate
Adjust gradient deviation values through the adaptive coefficient
Fusing the predicted gradient to form the composite gradient
$g_t$
$m_t$
Determine the gradient update mode
Determine the search direction at the next time
Update parameters
$\theta_t$

FIGURE 4: The architecture of ACGB-Adam.

```
Input: $\alpha, \beta_1, \beta_2, f_t$
Output: $\theta_t$
 (1)  Initialize parameters (adaptive coefficient $\beta_{1,t}$, predicted gradient $u_t$, and the remaining parameters were initialized in the same
      way as in the Algorithm 1)
 (2)    For $t = 1$ to $T$ do
 (3)        Generate a random diagonal matrix $D_t$/* Gradient Calculation based on Algorithm 2-RBC*/
 (4)        Get a stochastic gradient at time step $t$: $g_t = D_t \nabla_\theta f_t(\theta_{t-1})$
 (5)      Update the parameters according to the gradient descent method: $\theta_t = \theta_{t-1} - \alpha g_t$/ * Composite Gradient Optimization */
 (6)        Get a predicted stochastic gradient at time step $t$: $u_t = \nabla_\theta f_t(\theta_{t-1})$/* Optimization of the first moment estimation */
 (7)        Update biased first-order moment estimation: $m_t = \beta_{1,t} m_{t-1} + (1-\beta_{1,t})(g_t + u_t)$
 (8)        Update biased second-order moment estimation: $v_t = \beta_2 v_{t-1} + (1-\beta_2) {g_t}^2$
 (9)        Compute bias-corrected first-order moment estimation: $\widehat{m_t} = m_t/(1-\beta_{1,t}^t)$
(10)      Compute bias-corrected second-order moment estimation: $\widehat{v_t} = v_t/(1-\beta_2^t)$
(11)      Update the parameters: $\theta_t = \theta_{t-1} - \alpha \widehat{m_t}/\sqrt{\widehat{v_t}}$
(12)    End For
(13)  Return $\theta_t$
```

ALGORITHM 3: ACGB-Adam.

TABLE 2: Basic information of the Mnist and CIFAR-10 datasets.

| Datasets | Classes | Image type | Features | Number of training data | Number of test data |
|---|---|---|---|---|---|
| Mnist | 10 | Grayscale | 784 | 60000 | 10000 |
| CIFAR-10 | 10 | RGB | 3072 | 50000 | 10000 |

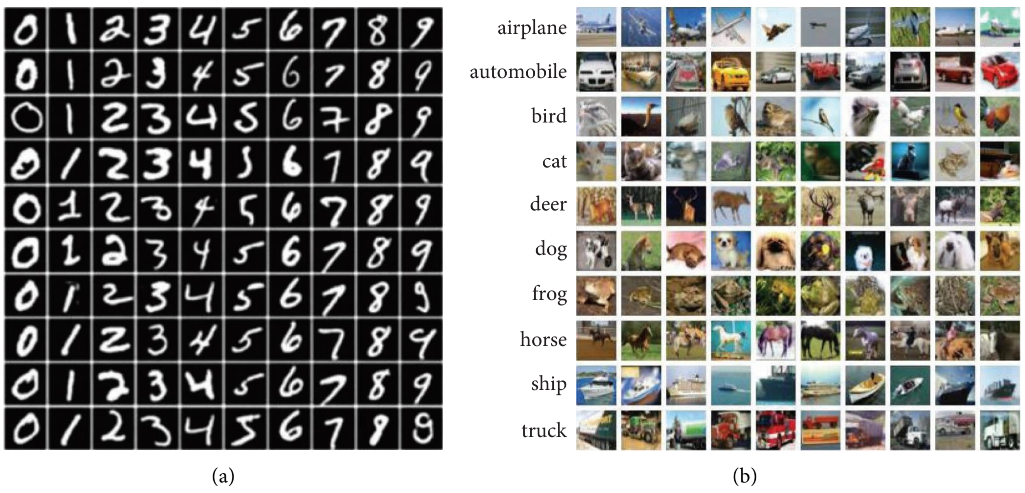

FIGURE 5: Samples of standard datasets: (a) Mnist dataset handwritten instances and (b) CIFAR-10 dataset picture category instances.

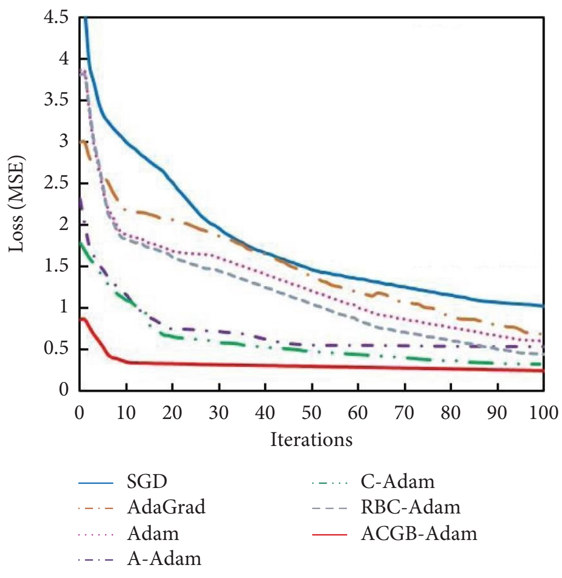

(a)

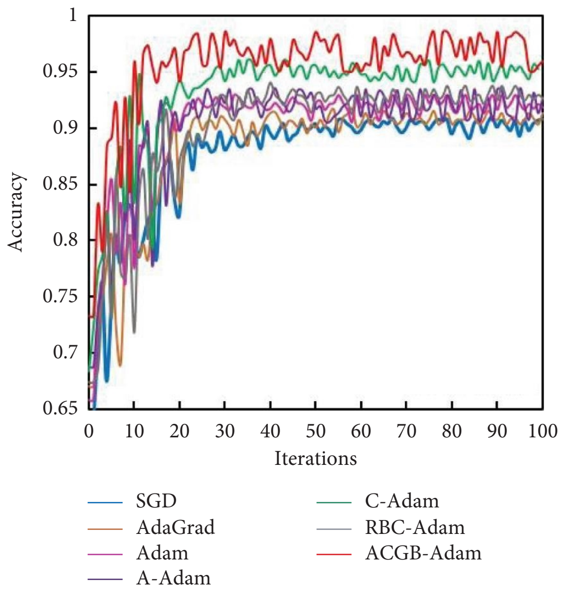

(b)

FIGURE 6: Experimental results of the Mnist dataset: (a) MSE and (b) accuracy.

TABLE 3: MSE and accuracy on Mnist dataset.

| Methods | SGD | AdaGrad | Adam | *A*-Adam | *C*-Adam | RBC-Adam | ACGB-Adam |
|---|---|---|---|---|---|---|---|
| MSE | 1.021 | 0.675 | 0.607 | 0.532 | 0.325 | 0.449 | 0.253 |
| Accuracy | 0.908 | 0.913 | 0.918 | 0.926 | 0.952 | 0.926 | 0.959 |

$$D_t = \begin{bmatrix} 1 & 0 & \cdots & 0 \\ 1 & 0 & \cdots & \vdots \\ \vdots & \vdots & \ddots & \vdots \\ 0 & \cdots & \cdots & 1 \end{bmatrix}. \tag{5}$$

The RBC method is used to randomly select a block (subset) from the whole element of a high-dimensional vector through equation (5) If $d_i^t = 1$, which means that the corresponding coordinates are selected, then the ACGB-Adam algorithm is executed for gradient calculation; if $d_i^t = 0$, which means that the corresponding coordinates are not selected, then the gradient update calculation is not performed. Thus, in each round of gradient updating, only one block (subset) of the gradient has to be computed, and the first-order and second-order momentum are calculated based on this. Moreover, it is not necessary to calculate the entire gradient. Therefore, compared with the other full gradient descent algorithms, the optimization method based on randomized block coordinate descent may save a lot of computing costs and reduce CPU utilization as well as memory utilization while ensuring the convergence of the algorithm. The specific calculation process is shown in Figure 3.

*3.4. ACGB-Adam Algorithm Process.* The ACGB-Adam algorithm process is described in the following sections.

*3.4.1. Overall Architecture of Algorithm.* The overall architecture of the ACGB-Adam algorithm is shown in Figure 4, which mainly includes three core modules: the random block coordinate method, the adjustment of gradient deviation values through adaptive parameters, and the composite gradient.

The general strategy of the ACGB-Adam algorithm is to integrate the above three modules and apply three optimization methods to solve problems in parameter updating so as to improve the convergence speed, global optimization ability and reduce the system overhead. First, the current gradient update mode is optimized by RBC, which can avoid calculating all gradients and reduce the system overhead. Secondly, through the adaptive parameters, the algorithm could calculate the coefficient proportion of the first momentum adaptively according to the difference between the current gradient and the first momentum at the last time so as to minimize the influence of the outlier gradient and optimize the search direction and search speed. Finally, the composite gradient combines the predicted gradient, the current gradient, and the first momentum of the last time to form the final search direction, aiming to further approach the global optimal position and improve the global search ability of the algorithm.

*3.4.2. ACGB-Adam Algorithm Process.* The overall algorithm flow of ACGB-Adam is shown in Algorithm 3.

## 4. Experiment and Analysis

The experiment and analysis are described in the following sections.

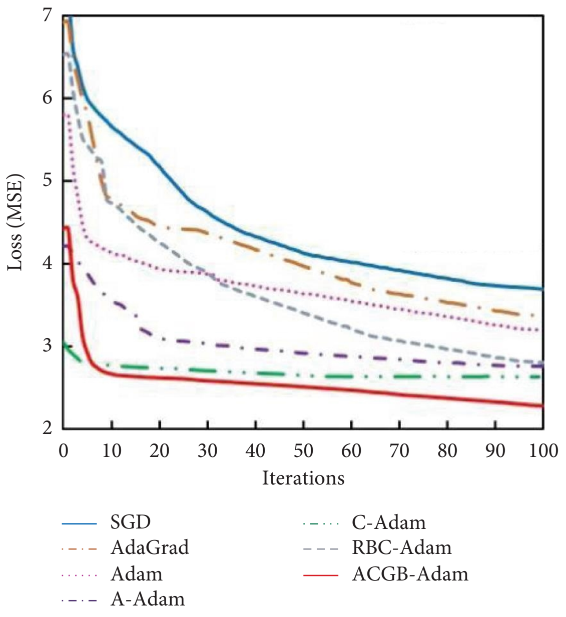

(a)

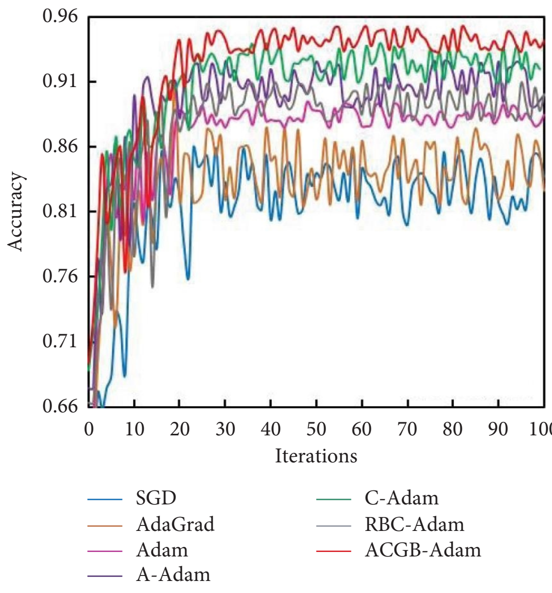

(b)

FIGURE 7: Experimental results of the CIFAR-10 dataset: (a) MSE and (b) accuracy.

TABLE 4: MSE and accuracy on the CIFAR-10 dataset.

| Methods | SGD | AdaGrad | Adam | *A*-Adam | *C*-Adam | RBC-Adam | ACGB-Adam |
|---|---|---|---|---|---|---|---|
| MSE | 3.690 | 3.364 | 3.191 | 2.757 | 2.635 | 2.798 | 2.287 |
| Accuracy | 0.837 | 0.826 | 0.885 | 0.90 | 0.92 | 0.901 | 0.941 |

*4.1. Standard Datasets and Experimental Setup.* To evaluate the performance of the ACGB-Adam algorithm, experiments were carried out on two standard datasets (Table 2) used for classification. The proposed algorithm was further compared with the stochastic gradient descent (SGD), the adaptive gradient (AdaGrad), the adaptive moment estimate (Adam), the Adam optimization algorithm based on adaptive coefficients (A-Adam), Adam optimization algorithm based on composite gradient (C-Adam), and Adam optimization algorithm based on randomized block coordinate descent (RBC-Adam) algorithms (Figure 5(a)).

(1) *Mnist Dataset*. The Mnist dataset [31] developed by the US postal system is a classic dataset for image recognition. In this dataset, 70000 digital pictures of 0~9 handwritten by 250 different people are counted. These numbers have been standardized in size and are located in the center of the image. Some examples of handwriting in the dataset are represented in Figure 5(a).

(2) *CIFAR-10 Dataset*. The CIFAR-10 dataset [32] is used for identifying universal objects which consists of 60000 RGB images. Compared with the handwritten characters, this dataset contains pictures of real objects in the real world. The noise is large, and the proportions and characteristics of objects are different, which lead to great difficulties in recognition. Figure 5(b) lists ten classes in the dataset, and each class shows ten pictures randomly.

(3) *Experimental Setting*. MATLAB is used for the simulation of experiments. The operating system is Win10, the CPU is Intel i7–1065G7, the primary frequency is 1.30 GHz, the memory is 16 GB, and the SSD capacity is 512 GB. To improve the comparability of the results, the six comparison algorithms involved in the experiment all use the same parameter settings. The main superparameters are as follows: $\alpha = 0.001$, $\beta_1 = \beta_2 = 0.9$, and the maximum number of iterations is 100. MSE and accuracy are used as performance evaluation indicators of algorithm training and classification accuracy.

*4.2. Experimental Results of the Standard Dataset.* The experimental results of the standard dataset are explained in the following sections.

*4.2.1. Mnist Experimental Results.* Figure 6 represents the training error loss and classification accuracy of the six algorithms on the Mnist. The training error and test accuracy at the 100th iteration are shown in Table 3. It can be observed from Figure 6 and Table 3 that, as the number of iterations increases, each algorithm gradually converges on the

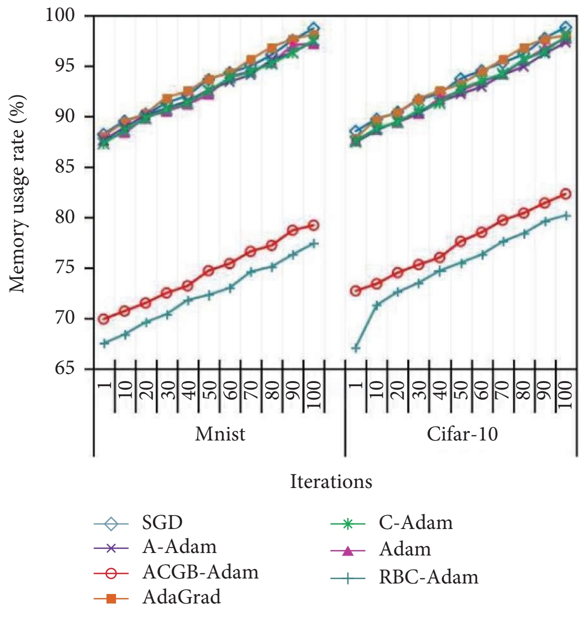

(a)

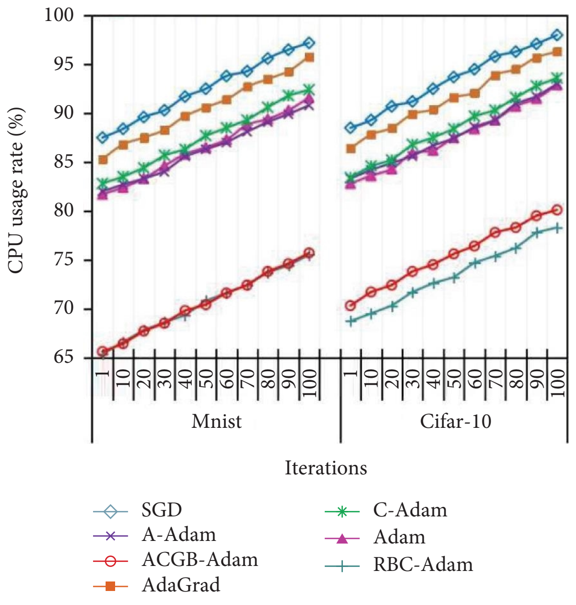

(b)

Figure 8: Change of (a) memory usage rate and (b) CPU usage rate with iterations.

Table 5: Comparison of the memory and CPU usage rate (%).

| | Dataset | SGD | AdaGrad | Adam | *A*-Adam | *C*-Adam | RBC-Adam | ACGB-Adam |
|---|---|---|---|---|---|---|---|---|
| Memory usage rate | Mnist | 98.7 | 98.1 | 97.2 | 97.4 | 97.5 | 77.4 | 79.2 |
| | CIFAR-10 | 98.8 | 98.0 | 97.7 | 97.3 | 97.9 | 80.2 | 82.3 |
| CPU usage rate | Mnist | 97.2 | 95.8 | 91.6 | 90.8 | 92.4 | 75.5 | 75.7 |
| | CIFAR-10 | 98.0 | 96.3 | 92.9 | 93.0 | 93.6 | 78.3 | 80.1 |

Table 6: Performance comparison of RBC-Adam and ACGB-Adam.

| | Dataset | MSE | Accuracy | Memory usage rate | CPU usage rate |
|---|---|---|---|---|---|
| RBC-Adam | Mnist | 0.449 | 0.926 | 77.4 | 75.5 |
| | CIFAR-10 | 2.798 | 0.901 | 79.2 | 82.3 |
| ACGB-Adam | Mnist | 0.253 | 0.959 | 80.2 | 78.3 |
| | CIFAR-10 | 2.287 | 0.941 | 82.3 | 80.1 |

training set, and the classification accuracy on the test set keeps improving. Compared with the other six algorithms, the ACGB-Adam algorithm quickly converges to the stable state, has the smallest error loss value, and has the highest classification accuracy of 0.959. This indicates that the algorithm proposed in this article has a good classification effect.

*4.2.2. CIFAR-10 Experimental Results.* Figure 7 demonstrates the training error of algorithms on the CIFAR-10 dataset, along with the classification accuracy of the test set. The training error and test accuracy at the 100th iteration are shown in Table 4. It can be observed from Figure 7 and Table 4 that the training error of the ACGB-Adam algorithm in the early stage of iterations reduces quickly and gradually tends to be stable. With the increase in iterations, the error loss of the algorithm still decreases steadily. Compared with the other six algorithms, the ACGB-Adam algorithm has the smallest error loss value and the highest classification accuracy of 0.941. From the experimental results on the CIFAR-10 dataset, it can be inferred that the proposed algorithm in this article has better optimization performance than the other six algorithms in terms of convergence speed, accuracy, stability, and classification accuracy.

*4.2.3. Memory and CPU Usage Rate Analysis.* For the two standard datasets, the changes in memory and CPU utilization of the seven algorithms with the number of iterations are illustrated in Figure 8 and Table 5.

It can be observed from Table 5 and Figure 8 that, with the increase of iteration times, the memory and CPU

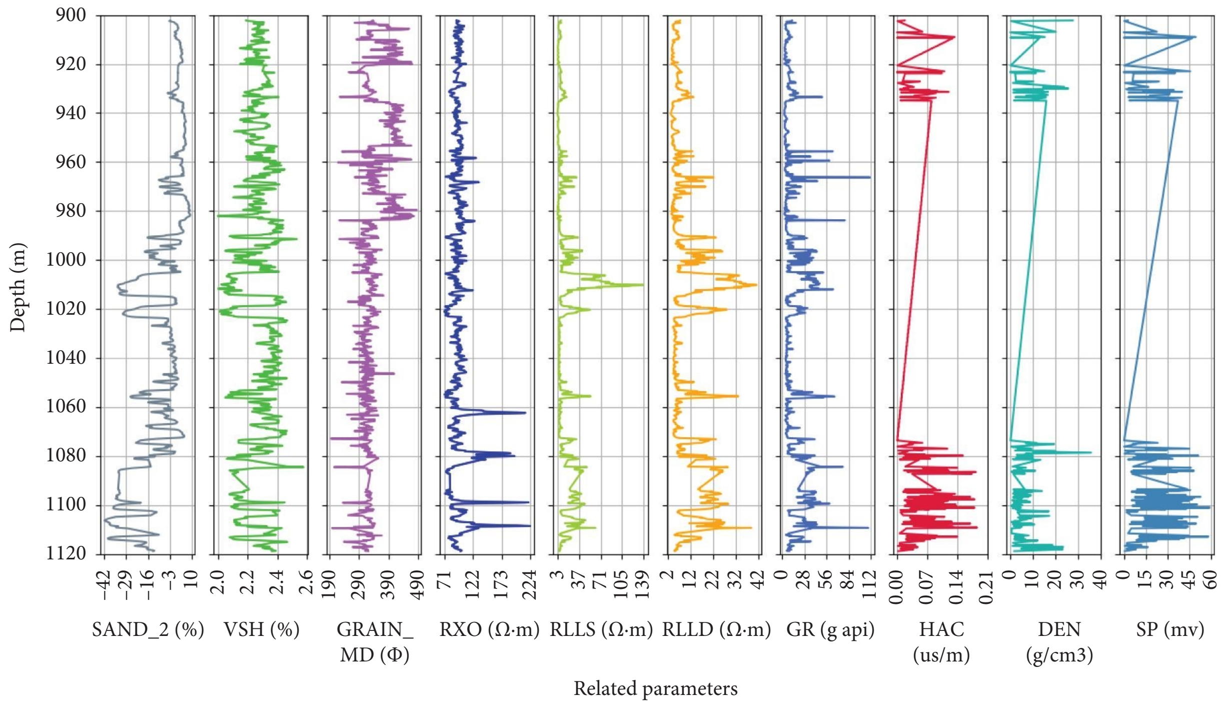

Figure 9: Distribution of sample data in the work.

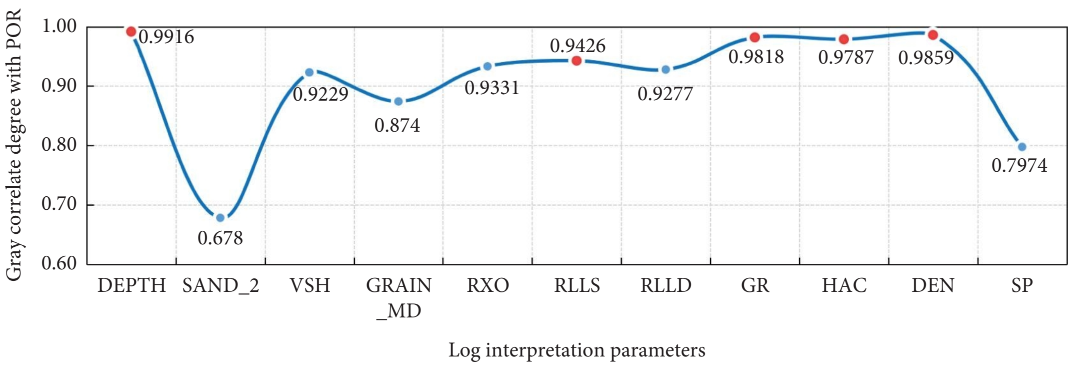

Figure 10: Gray correlation degree of the relevant parameters.

utilization of each algorithm increase gradually. Under the same conditions, the memory and CPU utilization of the RBC-Adam algorithm is the lowest, followed by the ACGB-Adam algorithm proposed in this article. The difference between the memory and CPU utilization rates of the two algorithms is less than 2%. The specific experimental results are shown in Table 6. It can be seen from Tables 5 and 6 that although the computing cost of the RBC-Adam algorithm is slightly lower than the ACGB-Adam algorithm, its training error and classification accuracy are far lower than those of the proposed algorithm. Altogether, the ACGB-Adam algorithm proposed in this article can achieve a dynamic balance in convergence and computing cost. On the premise of improving the convergence speed and accuracy, it can reduce the memory and CPU utilization to the greatest extent and has good comprehensive optimization performance.

### 4.3. Reservoir Porosity Prediction.

To further verify the effectiveness and utility of the algorithm proposed, the reservoir porosity in the real work area was predicted by a BP neural network based on the ACGB-Adam algorithm.

#### 4.3.1. Data Preparation and Preprocessing.

As shown in Figure 9, the sample data are from the real data of two wells, *A* and *B*, in an exploration area. The logging depth is 900~1120 m, including 1492 records and 11 logging parameters. To achieve efficient and accurate porosity prediction, the grey correlation analysis method [33] is used to select parameters with high correlation with porosity as input parameters of the neural network, namely, Depth, RLLS (shallow investigate double lateral resistivity log), GR (natural gamma ray), HAC (high-resolution interval transit time), and DEN (density), as represented in Figure 10. This

Table 7: Training error and test error of six methods.

| | Training error | | | | | |
|---|---|---|---|---|---|---|
| | SGD_BP | AdaGrad_BP | Adam_BP | *C*-Adam_BP | RBC-Adam_BP | ACGB-Adam_BP |
| MSE | 1.174293 | 0.51372 | 0.095824 | 0.021837 | 0.101693 | **0.019725** |
| RMSE | 1.083648 | 0.716743 | 0.309555 | 0.147773 | 0.318893 | **0.140446** |
| | Test error | | | | | |
| | SGD_BP | AdaGrad_BP | Adam_BP | *C*-Adam_BP | RBC-Adam_BP | ACGB-Adam_BP |
| MSE | 1.267104 | 0.566655 | 0.163862 | 0.028447 | 0.155603 | **0.022442** |
| RMSE | 1.125657 | 0.752772 | 0.404799 | 0.168662 | 0.394465 | **0.149807** |

The minimum values of MSE and RMSE in Table 7 is shown in bold.

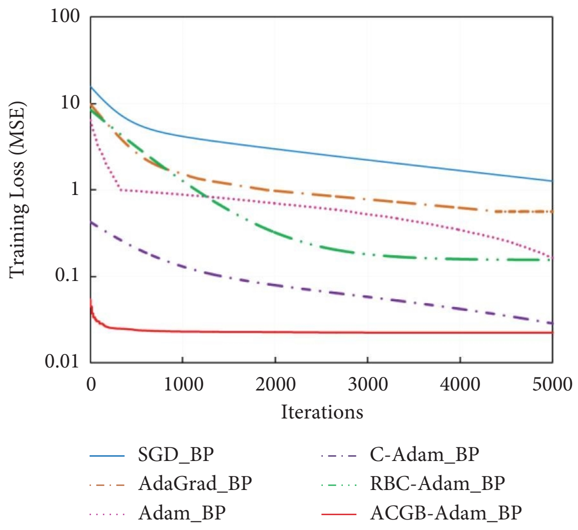

Figure 11: The iterative curves of the methods.

helps to improve the data processing efficiency on the premise of ensuring prediction accuracy.

It can be assumed that these five parameters that have a significant impact on porosity are different in nature and usually have distinct dimensions and orders of magnitude. In case the level difference between the parameters is too large, the influence of the parameters with higher values will be highlighted, and the effect of the parameters with lower values will be weakened. To ensure the comparability of the data, this article uses the deviation normalization method [33] to preprocess the data and eliminates the influence of the dimension and the value of the variable itself on the results.

*4.3.2. Model Performance Analysis.* The preprocessed data were taken as sample data, and the training set and test set were divided in the ratio of 8 : 2. The BPNN model is set as follows: the number of hidden layers was 1, including 5 neurons, the transfer function was Tansig, the learning rate was 0.001, and the maximum number of iterations was 5000. Using MSE and RMSE as the model performance evaluation indices, the proposed ACGB-Adam_BP model was compared with five methods, namely, SGD_BP, AdaGrad_BP, Adam_BP, *C*-Adam_BP, and RBC-Adam_BP. The final training error and test error of various methods are enlisted in Table 7, in which the minimum values of MSE and RMSE are shown in bold, and the iterative error curve is shown in Figure 11.

It can be seen from Table 7 and Figure 11 that the BPNN based on the ACGB-Adam algorithm generates the lowest error in the training set and the test set and tends to be stable as soon as possible. The convergence speed is much better than the other five comparison algorithms. This indicates that the proposed algorithm has better optimization performance.

*4.3.3. Porosity Prediction Results.* To further observe the above results intuitively and validate the effectiveness and correctness of the method proposed in this article for porosity prediction, the prediction results of the BP model based on the ACGB-Adam optimization algorithm are visually analyzed in terms of 300 test samples, as highlighted in Figure 12. Due to space constraints, the error analysis results on the training set are not shown in the article. From the comparison curve between the predicted value and the actual value of porosity, it can be observed that the BP neural network model based on the ACGB-Adam optimization algorithm has a relatively ideal prediction result, and the predicted abnormal value of porosity is quite less. The absolute error of more than 86% of the data is

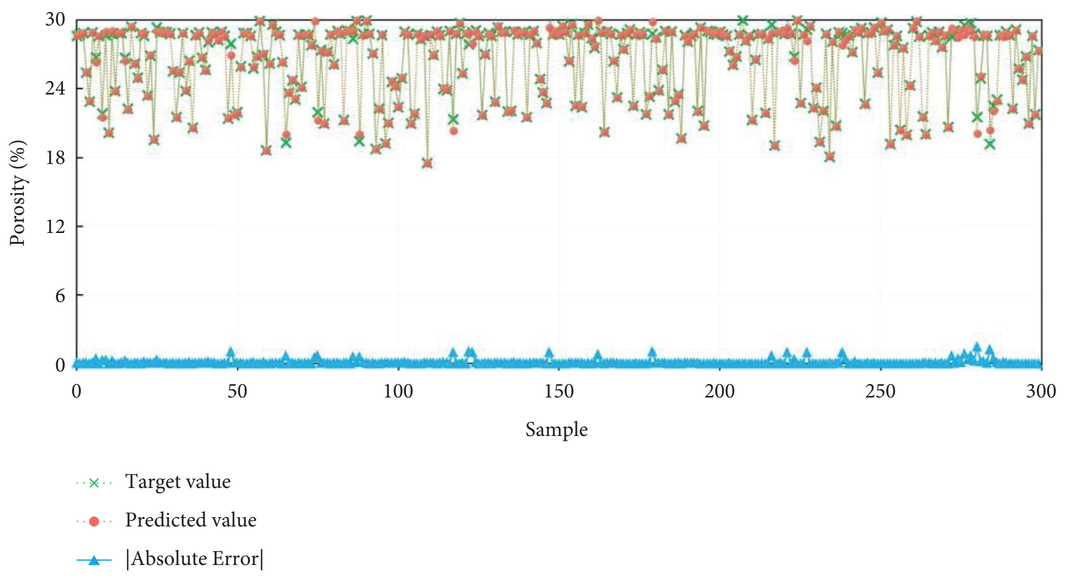

Figure 12: Porosity prediction results based on the ACGB-Adam_BP method.

within 0.1%, which signifies the high prediction accuracy of the proposed algorithm.

## 5. Conclusion

Starting with the improvement of the Adam algorithm to heighten the convergence speed, accelerating the search for the global optimal solution, and enhancing the high-dimensional data processing ability, the Adam optimization algorithm combining adaptive coefficients and composite gradients based on randomized block coordinate descent is proposed, which enhances the performance of the algorithm. Through theoretical analysis and numerical experiments, the following conclusions can be drawn:

(1) The gradient deviation caused by the outliers is crucial to the convergence speed and solution precision of the Adam algorithm. Using an adaptive coefficient to adjust the difference between the first-order momentum and the current gradient can help in reducing the influence of parameter proportion of deviation gradient, improving the slow convergence speed of the Adam algorithm, boosting the search speed, and improving the convergence accuracy.

(2) By introducing the prediction gradient and combining the current gradient and the first-order momentum to form a composite gradient, an accurate search direction can be obtained in the subsequent iteration, and then, the global optimization ability of the algorithm could be enhanced.

(3) In the process of gradient updating, the RBC method is used to determine the gradient calculation method by randomly selecting variables from the parameter subset. This can reduce the calculation cost as much as possible on the premise of ensuring the convergence of the algorithm, enhance the processing ability of the algorithm for high-dimensional data, and maintain a good balance between the optimization accuracy and the system overhead.

(4) The test results on Mnist and CIFAR-10 standard datasets for classification indicate that the ACGB-Adam algorithm is significantly superior to SGD, AdaGrad, Adam, *A*-Adam, *C*-Adam, and RBC-Adam algorithms in terms of convergence speed and optimization accuracy. Although the proposed method is slightly higher than the RBC-Adam algorithm in terms of memory and CPU utilization, it can achieve a decent balance between convergence and system overhead. According to the evaluation indices, the proposed algorithm has better performance advantages compared with the other five algorithms, which validates the effectiveness of the algorithm improvement.

(5) The BPNN model based on the ACGB-Adam algorithm is applied to reservoir porosity prediction. The experimental results suggest that, as compared to the BPNN model based on Adam and its variants, the maximum reduction of MSE and RMSE of the proposed model in this article is approximately 86.30% and 62.99%, respectively, which achieves higher accuracy in porosity prediction, verifies the superiority of the proposed algorithm, and extends the application field of the algorithm.

The method proposed in this article enhances the performance of the Adam optimization algorithm to a certain extent, but does not consider the impact of the second-order momentum and different learning rates on the performance of the original algorithm. Therefore, the follow-up research can focus on the optimization and improvement of the second-order momentum and learning rate and conduct in-depth and detailed research on the parts not involved in this algorithm. This can help to attain better optimization performance.

## Data Availability

No data were used to support the findings of the study.

## Conflicts of Interest

The authors declare that they have no conflicts of interest.

## Acknowledgments

This work was supported by the National Natural Science Foundation of China (Grant nos. 42002138 and 62172352), Natural Science Foundation of Heilongjiang Province (Grant no. LH2020F003), Postdoctoral Scientific Research Development Fund of Heilongjiang Province (Grant no. LBH-Q20073), Excellent Young and Middle-aged Innovative Team Cultivation Foundation of Northeast Petroleum University (Grant no. KYCXTDQ202101), and S&T Program of Hebei (Grant no. 226Z0102G).

## References

[1] Z. Pan, D. Lei, and L. Wang, "A Knowledge-Based Two-Population Optimization Algorithm for Distributed Energy-Efficient Parallel Machines Scheduling," *IEEE Transactions on Cybernetics*, vol. 52, 2020.

[2] J. J. Wang and L. Wang, "A cooperative memetic algorithm with feedback for the energy-aware distributed flow-shops with flexible assembly scheduling," *Computers & Industrial Engineering*, vol. 168, Article ID 108126, 2022.

[3] L. Bottou, "Large-scale machine learning with stochastic gradient descent," *Proceedings of the COMPSTAT' 2010*, pp. 177–186, Paris, France, August, 2010.

[4] N. Qian, "On the momentum term in gradient descent learning algorithms," *Neural Networks*, vol. 12, no. 1, pp. 145–151, 1999.

[5] M. Wang, S. Zhou, Z. Yang, Z. Liu, and S. Ren, "A brief introduction to deep learning technology," *Automation technology and application*, no. 5, pp. 18–25, 2019.

[6] I. Goodfellow, Y. Bengio, and A. Courville, *Deep Learning*, MIT Press, Cambridge, MA, USA, 2016.

[7] J. R. Sashank, K. Satyen, and K. Sanjiv, "On the convergence of adam and beyond," in *Proceedings of the International Conference on Learning Representations*, Vancouver, BC, Canada, April, 2018.

[8] J. Ma and D. Yarats, "Quasi-hyperbolic momentum and adam for deep learning," in *Proceedings of the 7th International Conference on Learning Representations, ICLR*, New Orleans, LA, USA, May, 2019.

[9] L. Luo, Y. Xiong, Y. Liu, and X. Sun, "Adaptive gradient methods with dynamic bound of learning rate," in *Proceedings of the 7th International Conference on Learning Representations, ICLR*, New Orleans, LA, USA, May, 2019.

[10] M. Yin, Y. Wang, Z. Sun, and Y. Yu, "A compound gradient accelerated optimization algorithm with adaptive step size," *Journal of Northeastern University: Natural Science Edition*, vol. 41, no. 9, p. 6, 2020.

[11] K. S. Kim and Y. S. Choi, "HyAdamC: a new adam-based hybrid optimization algorithm for convolution neural networks," *Sensors*, vol. 21, no. 12, p. 4054, 2021.

[12] D. John, H. Elad, and Y. Singer, "Adaptive subgradient methods for online learning and stochastic optimization," *Journal of Machine Learning Research*, no. 12, pp. 2121–2159, 2011.

[13] M. Zaheer, S. Reddi, D. Sachan, S. Kale, and S. Kumar, "Adaptive methods for nonconvex optimization," in *Proceedings of the 32nd International Conference on Neural Information Processing Systems*, pp. 9815–9825, Montreal, Canada, December 2018.

[14] J. Bernstein, A. Vahdat, Y. Yue, and M. Y. Liu, "On the Distance between Two Neural Networks and the Stability of learning," in *Proceedings of the 34th Conference on Neural Information Processing Systems (NeurIPS 2020)*, Vancouver, Canada, February, 2020.

[15] S. R. Dubey, S. Chakraborty, S. K. Roy, S. Mukherjee, and B. B. Chaudhuri, "diffGrad: an optimization method for convolutional neural networks," *IEEE Transactions on Neural Networks and Learning Systems*, vol. 31, no. 11, pp. 4500–4511, 2020.

[16] Y. Zhou, M. Zhang, J. Zhu, Q. Zheng, and Q. Wu, "A Randomized Block-Coordinate Adam online learning optimization algorithm," *Neural Computing & Applications*, vol. 32, no. 16, pp. 12671–12684, 2020.

[17] W. E. L. Ilboudo, T. Kobayashi, and K. Sugimoto, "Robust stochastic gradient descent with student-t distribution based first-order momentum," *IEEE Transactions on Neural Networks and Learning Systems*, vol. 33, no. 3, pp. 1324–1337, 2022.

[18] Brownlee and J. Better, *Deep Learning: Train Faster, Reduce Overfitting, and Make Better Predictions Machine Learning Mastery*, San Juan, PR, USA, 2018.

[19] D. Kingma and J. Ba, "Adam: a method for stochastic optimization," *Computer Science*, 2014.

[20] S. Ruder, "An overview of gradient descent optimization algorithms," 2016, https://arxiv.org/abs/1609.04747.

[21] T. Dozat, "Incorporating nesterov momentum into adam," in *Proceedings of the International Conference on Learning Representations(ICLR)*, San Juan, Puerto Rico, May 2016.

[22] J. Zhang and F. B. Gouza, "GADAM: Genetic-evolutionary adam for deep neural network optimization," 2018, https://arxiv.org/abs/1805.07500.

[23] S. J. Reddi, S. Kale, and S. Kumar, "On the convergence of adam and beyond," 2019, https://arxiv.org/abs/1904.09237.

[24] N. Shazeer and M. Stern, "Adafactor: Adaptive learning rates with sublinear memory cost," in *Proceedings of the International Conference on Machine Learning ICML*, pp. 4596–4604, Stockholm, Sweden, July 2018.

[25] M. Zaheer, S. J. Reddi, and D. S. Sachan, "Adaptive methods for nonconvex optimization," in *Proceedings of the Neural Information Processing Systems*, Curran Associates, Inc, Montreal, Canada, December 2018.

[26] Z. Lu and X. Lin, "Randomized block coordinate non-monotone gradient method for a class of nonlinear programming," 2013, https://arxiv.org/abs/1306.5918.

[27] E. L. Hu and J. T. Kwok, "Scalable nonparametric low-rank kernel learning using block coordinate descent," *IEEE Transactions on Neural Networks and Learning Systems*, vol. 26, no. 9, pp. 1927–1938, 2015.

[28] T. Zhao, M. Yu, Y. Wang, and L. Arora, "Accelerated mini-batch randomized block coordinate descent method," *Advances in Neural Information Processing Systems*, vol. 27, p. 5614, 2014.

[29] C. Singh, A. Nedic, and R. Srikant, "Random block-coordinate gradient projection algorithms," in *Proceedings of the IEEE Conference on Decision and Control*, pp. 185–190, Los Angeles, CA, USA, December, 2014.

[30] T. Y. Xie, B. Liu, Y. Xu et al., "A block coordinate ascent algorithm for mean-variance optimization," in *Proceedings of the Neural Information Processing Systems NIPS*, pp. 1073–1083, Convention center in Montreal, Canada, December 2018.

[31] L. Li Deng, “The MNIST database of handwritten digit images for machine learning research [best of the web],” *IEEE Signal Processing Magazine*, vol. 29, no. 6, pp. 141-142, 2012.

[32] D. Bankman, L. Yang, B. Moons, M. Verhelst, and B. Murmann, “An always-on 3.8$\mu$J/86% CIFAR-10 mixed-signal binary CNN processor with all memory on chip in 28nm CMOS,” in *Proceedings of the 2018 IEEE International Solid - State Circuits Conference - (ISSCC)*, IEEE, San Francisco, CA, USA, February, 2018.

[33] M. Liu, D. Yao, J. Guo, and J. Chen, “An optimized neural network prediction model for reservoir porosity based on improved shuffled frog leaping algorithm,” *International Journal of Computational Intelligence Systems*, vol. 15, no. 1, pp. 1–19, 2022.